International Journal of Innovative Research in Advanced Engineering (IJIRAE) ISSN: 2349-2163
Issue 06, Volume 4 (June 2017) www.ijirae.com

Measuring Cardiac Contraction Velocity Using M-Mode Ultrasonography with Digital Image Processing

Niken Larasati *, Suryono, Kusworo Adi*****
**Physics Graduate Program, Diponegoro University, Kota Semarang, Indonesia*
nikenlrst@st.fisika.undip.ac.id
***, ***Physics Department, Diponegoro University*, Kota Semarang, *Indonesia*
suryono@undip.ac.id, kusworoadi@undip.ac.id

Manuscript History
Number: IJIRAE/RS/Vol.04/Issue06/JNAE10085
Received: 27, April 2017
Final Correction: 19, May 2017
Final Accepted: 27, May 2017
Published: June 2017
Citation: Larasati, N.; Suryono & Adi, K. (2017), 'Measuring Cardiac Contraction Velocity Using M-Mode Ultrasonography with Digital Image Processing', Master's thesis, Diponegoro University, Kota Semarang, Indonesia.
Editor: Dr.A.Arul L.S, Chief Editor, IJIRAE, AM Publications, India

Abstract— *Measurement of cardiac contraction velocity using M-mode ultrasonography with the help of digital image processing has been carried out. Analysis of organ movement rate is of great importance in medical imaging as it relates to diagnosis for diseases. This research is aimed at measuring the rate of heart contraction using digital image processing that employs the active contour segmentation method. The sample used is a video of cardiac check using M-mode USG that lasts 30 seconds and has a frame rate of 30 frames/seconds. This image was then extracted as to get 900 USG images each at 480 x 360 pixels. Measurement of the edges of cardiac images was conducted using MATLAB software. Results show that the cardiac in the video shifted farthest at 73/30 seconds, to 10.34 mm against the x-axis and at 28/30 seconds, to 14.00 mm from the y-axis. Meanwhile, the contraction velocity fluctuated.*

Keywords— *Velocity, Cardiac, USG Image, Digital Image Processing*

I. INTRODUCTION

Analysis of organ movement velocity is of great importance in medical imaging as it relates to diagnosis for diseases. Shifts in motion velocity can also be used to compress digital images using blocks based on motion estimation techniques [7]. Measuring organs' motion velocity is necessary in order to know the position of certain organs at particular times, as this also relates to the proper therapy the organs may need [17].

Over the past few years there have been studies concerning analyses of organ motion velocity. Organ motion measurement is used in the analysis of breast deformation to know tissue elasticity and provide indications for tissue stiffness by calculating the images' relative strain and young modulus [10]. Some elasticity imaging techniques have also been developed to quantitatively measure tissue elasticity with the help of ultrasound. Examples for these include detection and diagnosis of cancer in breast, prostate, and liver. Other examples include related clinical applications that measure the elastic property of soft tissues. Hence, the development of elastography USG took place. This technique shows great promise due to its real-time ability and its ease of use. Elastography USG, when it comes to B-mode sonography, proves to be a reliable method in confirming benign breast lesion. Moreover, differentiation of malignancy category using elastography equals to that using conventional USG [12].

Ultrasonography is also utilized in estimating and visualizing longitudinal movements of muscles [11]. USG is used in velocimetry imaging of human vitreous as well [18]. In 2007, USG was used to measure the velocity of blood flow using two methods of cross-correlation and de-correlation [16].

Ultrasound is considered the cheapest method of all. This shows its routine use in hospitals and clinics to diagnose all sorts of diseases. This is the instrument of choice for midwifery and cardiology due to its safety and real-time image processing ability. Nowadays, USG images are already in the form of digital image known as Digital Image Communication in Medicine (DICOM). Each digital image has its own blurring level that may affect an image's sharpness [6]. Generally, a digital image comes with noise that requires image processing for its improvement, as to allow proper interpretation.

II. METHOD

The research was carried out at the Instrumentation and Electronics Laboratory of the Faculty of Science and Mathematics in Diponegoro University, Semarang. Analyses were made on a video of a cardiac check using M-mode USG with the help of a PC equipped with MATLAB R2014b.

The procedures involved were; video extraction, image segmentation, morphology operation, determination of image spatial resolution, and graphical analyses. Extraction was carried out on a video of a cardiac check that lasts 30 seconds and with a frame rate of 30 frames/second. This process yielded 900 images of 480 x 360 pixel. From these, the number to be analyzed was 150, or the cardiac contraction for the first 5 seconds.

Image segmentation is the processing of images that separates the region of the object with that of its background, as to make it easier to do analyses. This is necessary as object recognition requires a lot of visual perceptions. The segmentation method done here includes; active contouring, which a segmentation method is using a loop curve that can either narrows or expands [4].

The initial process of this stage is by determining the initial masking, represented in a loop curve and then iteratively modifying this mask that will allow the narrowing and expanding operation until a desired object shape is obtained, as depicted in Figure 1.

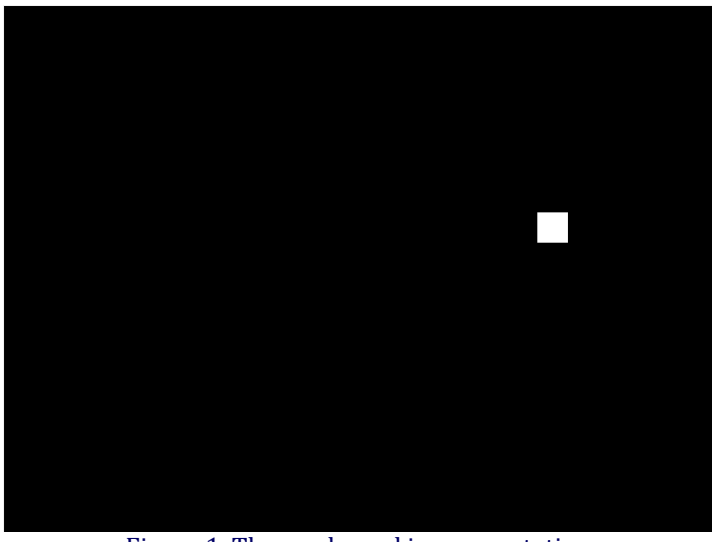

Figure 1. The mask used in segmentation

Measurement of spatial resolution is carried out by calculating the number of pixels within a 10 mm distance. This research analyzed two dimensional cardiac contraction. Therefore, the upper horizontal edge is taken as the x-axis, and the vertical edge of the image is taken as the y-axis. Subsequently, two graphs will be analyzed; the graph between the edge of the heart to the x-axis, and the graph between the edge of the heart to the y-axis.

The first step to do is determining a random point in the x and y axis as a reference. This reference for the x-axis is at point 360 and for the y-axis is at point 150. The next step is to draw a line from the reference point to the edge of the cardiac image and then measure its distance. Once the distance is known, the following step is plotting this distance data against time in a graph. The flow chart of the research is given in Figure 2 as follows:

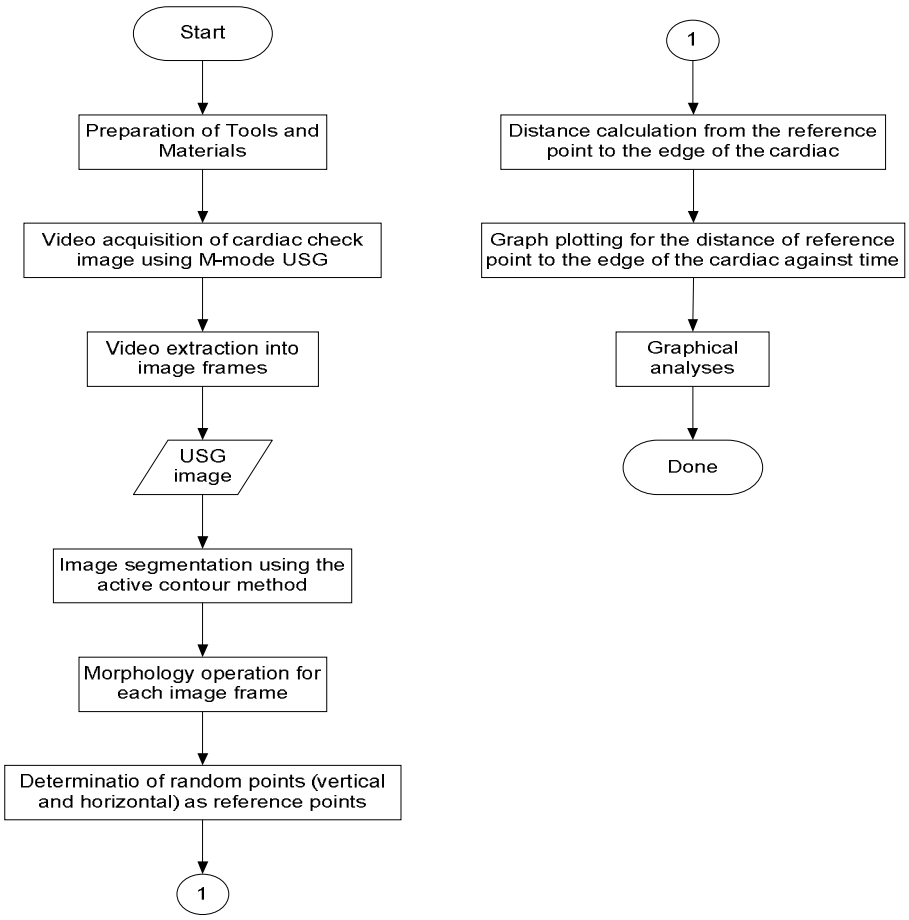

Figure 2. Research Flow Chart

III. RESULT AND DISCUSSION

Segmentation is aimed at separating the object region from the background area as to make it easier for object analysis using visual perception. This process involves the use of the loop curve model that can either narrows or expands by minimizing image energy using external force. This process is also influenced by the image's characteristics such as line or edge.

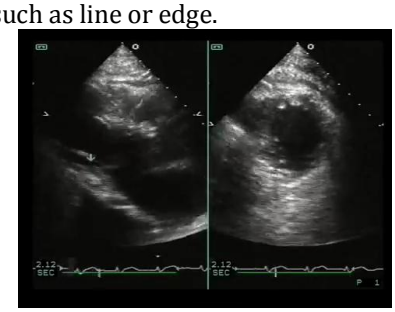

(a) Original image

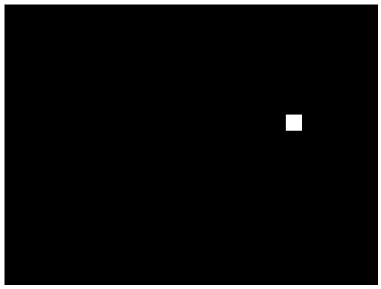

(b) The mask used

(c) Result of active contouring segmentation

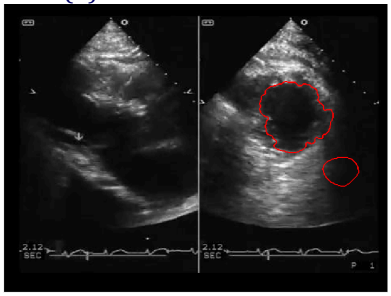

(d) Visual of segmentation result

Figure 3. Segmentation process using the active contouring method on frame 1

Figure 3 depicts results of active contouring on the image at frame 1. Figure 3(a) shows the original image from video grabbing of a cardiac check image that used M-mode USG in frame 1. Figure 3(b) is the mask used in the segmentation process using active contour. The mask can either narrows or expands in line with the cardiac image. Figure 3(c) reveals result of active contouring of the cardiac image. Figure 3(d) depicts result of active contouring for the heart visualized on the first frame of the cardiac image.

Figure 4 shows result of active contouring on frame 55. Like in Figure 4, Figure 4(a) depicts the real image from video grabbing from the image of a cardiac check using M-mode USG on frame 55. 4(b) is the mask used in active contouring segmentation. The mask can either narrows or expands in line with the cardiac image. Figure 4(c) reveals result of active contouring of the cardiac image. Figure 4(d) depicts result of active contouring of the cardiac image visualized on frame 55 of the cardiac image.

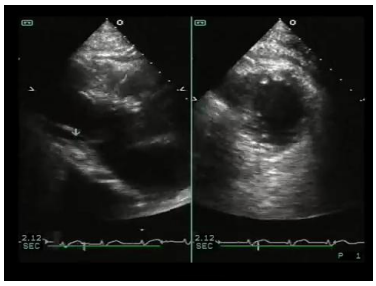

(a) Original image

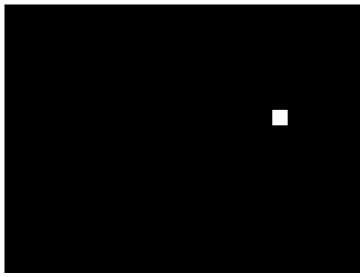

(b) The mask used

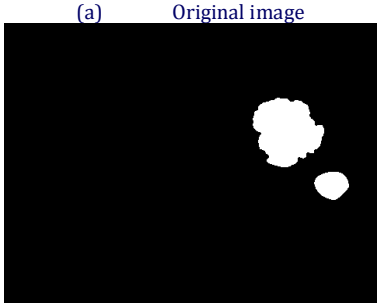

(c) Result of active contouring segmentation

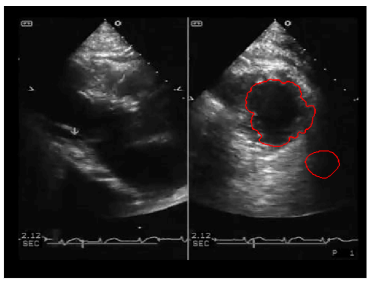

(d) Visual of segmentation result

Figure 4. Segmentation process using the active contouring method on Frame 55

The subsequent step is conducting morphological operation on segmentation results. This process is aimed at making up for the lacks from segmentation. The operation employed here is known as areal opening. Results of this operation are the loss of smaller objects without compromising the area of the target object. After some trials and errors, it is determined that the area of more than 2750 is considered the cardiac image and the area less than this value is going to be erased.

Figure 3(a) shows result of active contouring segmentation of the cardiac image on frame 1. Figure 3(b) is Figure 3(a) after undergoing morphology operation. Both pictures do not reveal any differences as there is no noise on frame 1. Meanwhile, Figure 4(a) shows result of active contouring segmentation of the cardiac image on frame 55. Unlike frame 1, there is noise on frame 55, just below the cardiac image. Once morphology is carried out, the noise is gone and the leftover is the cardiac image as depicted in Figure 4(b).

(a)Result of active contouring segmentation

(b)Result of morphology operation

Figure 5. Morphology operation on frame 1

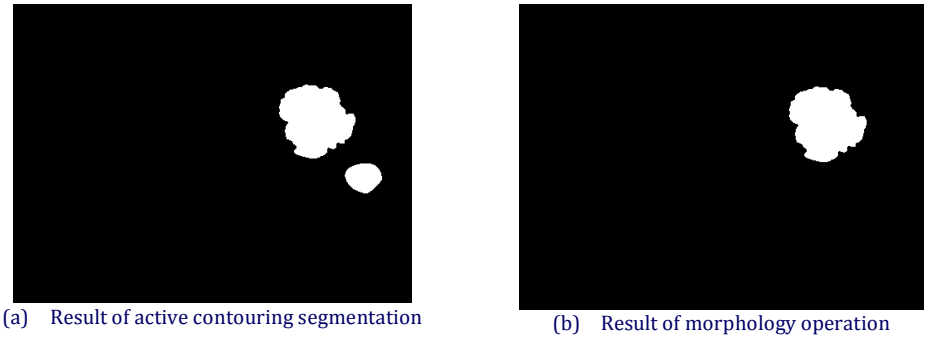

(a) Result of active contouring segmentation (b) Result of morphology operation

Figure 6. Morphology operation on frame 55

CALCULATION OF IMAGE SPATIAL RESOLUTION

Measurements show that within a 10 mm distance, there are 15 pixels. The magnitude of image spatial resolution of USG probe can be known from the following formula:

$$\text{Spatial resolution} = \frac{numberofpixel}{dis\tan ce(mm)}$$

$$= \frac{15\,pixel}{10mm}$$

$$= 1.5 \text{ pixels per mm}$$

Once measurement of the cardiac edge against the x-axis from frame 1 to frame 150 is done, distance for each frame is calculated to figure out the distance covered in 1/30 seconds. Results of calculation of the distance covered by the cardiac against time on the x-axis are given in Figure 7. The reference point use is x = 360 mm. It can be seen in Figure 7 that some points show the cardiac does not shift from its position. The cardiac has maximum contraction at 73/30 seconds, for as far as 10.34 mm.

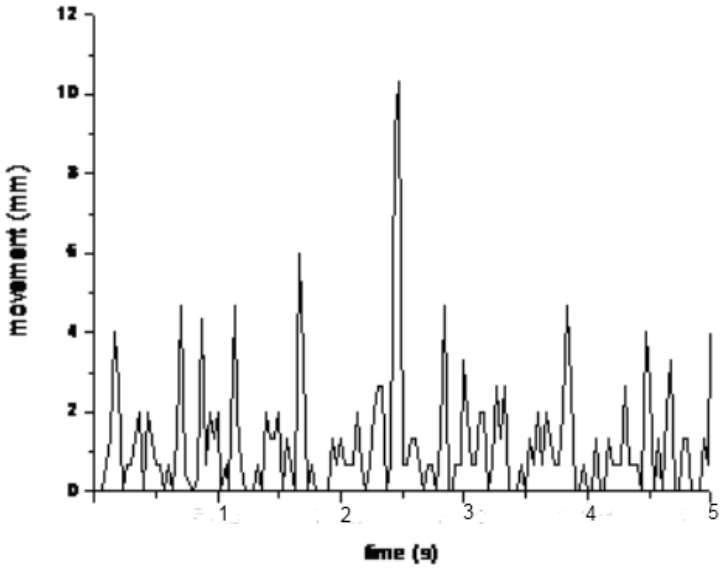

Figure 7. The distance covered by the cardiac (mm) against time (s) on the x-axis

Results of measurement for the distance covered by the cardiac against time on the y-axis are given in Figure 8. The reference point used is at y = 150 mm. It can be seen in Figure 8 that some points are of 0 (zero) value, which indicates no displacement. The farthest shift takes place on the 28/30 seconds, for as far as 14.00 mm. Measurements of distance on the y-axis does not reveal any contraction pattern as is the case for the x-axis. Therefore, the average contraction velocity cannot be calculated.

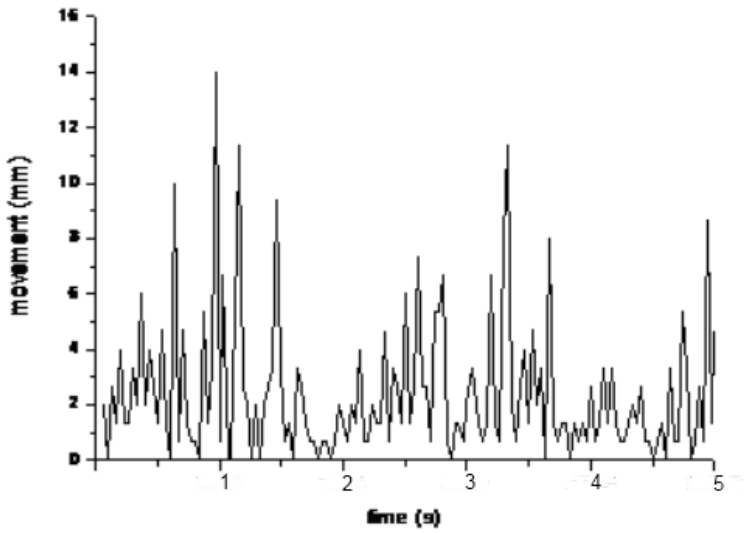

Figure 8. The distance covered by the cardiac (mm) against time (s) on the y-axis

IV. CONCLUSIONS

It can be inferred from the results here that cardiac contraction fluctuates in its rate. The cardiac studied here has the farthest shift on 73/30 seconds, for as far as 10.34 mm on the x-axis, and on the 28/30 seconds, for as far as 14.00 mm on the y-axis.

REFERENCES

1. Burns, P.N, 2005, Introduction to the Physical Principles of Ultrasound Imaging and Doppler, Journal Medical Biophysics-MBP1007/1008, pp 5.
2. Bushberg, J., T., and J. Anthony S., 2002, The Essential Physics of Medical Imaging, second edition, Philadelphia, USA, Lippincott Williams & Wilkins.
3. Cameron, J., R., and Skofronick, J.G, 1978, Medical Physics, pp 253-287, John Wiley and Sons Inc., New York.
4. Casseles, V., Kimmel R. and Sapiro G., 1997, Geodesic Active Contour. International Journal of Computer Vision.
5. Destyningtias B., Heranurweni S. and T. Nurhayati. 2010. Segmentasi Citra dengan Metode Pengambangan. Jurnal Elektrika. Vol.2, No.1, 2010: 39 – 49.
6. Dougherty, G., 2009, Digital Image Processing for Medical Applications, Cambridge University Press, New York.
7. Gao, L., K. J. Parker, R. M. Lerner, and S. F. Levinson, 1996, Ultrasound Medical Biology, pp. 959–977.
8. Goodsitt, M.M., and Carson, P.L, 1998, Real-time B-mode ultrasound quality control test procedures, Report of AAPM Ultrasound Task Group No.1, Department of Radiology, University of Michigan.
9. Kist, W.J., 2011, Sonography-Based Automated Volume Count to estimate fetal urine production in twin-to-twin transfusion syndrome, comparison with Virtual Organ Computer-aided analysis, American Journal of Obstetrics Gynecol, Leiden University Medical Center, Leiden, The Netherlands.
10. Kontogeorgakis, C., M. G. Strintzis, N. Maglaveras, and I. Kokkinidis, 1994, Tumor Detection in Ultrasound B-mode Image Through Estimation Using Texture Detection Algorithm, Proceedings 1994 Computer Cardiology Conference, pp. 117–120.
11. Li, Jizhou, 2013, Estimation and Visualization of Longitudinal Muscle Motion Using Ultrasonography: A feasibility study, Ultrasonic 54 (2014) 779–788.
12. Lu, Minhua, 2014, A Real Time Displacement Algorithm for Ultrasound Elastography, COMIND-2613; No. of Pages 11.
13. Maysanjaya, I., and M.Dendi, 2013, Pengembangan system identifikasi jenis kelamin janin pada citra USG, ISSN 2089-8673, ,Volume 2, Nomor 1, Jurnal Nasional Pendidikan Teknik Informatika (JANAPATI).
14. Munir, R., 2004, Pengolahan Citra Digital dengan Pendekatan Algoritma, Penerbit Informatika, Bandung.
15. Osman, M.Y., and Tahab F.A., 2005, Quality Control Program of Real Time Medical Ultrasound Machines In Sudan, Sudan Atomic Energy commission, Khartoum, Department of Applied Physics, Faculty of Applied sciences, Sudan.

16. Pan, T., and Huihua Kenny Chiang, 2007, Ultrasound Low-Velocity Flow Estimations Using Cross-Correlation and Decorrelation: A thread phantom study, Medical Engineering & Physics 29 (2007) 602–614.
17. Ranjit ,S.S., A.F. Tuani Ibrahim, S.I. Salim and S.K. Subramaniam, 2009, Analysis of Motion Velocity in Ultrasounds Image, International Journal of Video & Image Processing and Network Security Vol: 9 No: 9.
18. Rossi, T., and Giorgio Querzoli, 2012, Ultrasound Imaging Velocimetry of The Human Vitreous, Experimental Eye Research 99 (2012) 98e104.
19. Smith, S.W., 1999, The Scientist and Engineer's Guide to Diginal Signal Processing Second Edition, California Technical Publishing, California.
20. Tole, N.M. and Ostensen, H., 2005, Basic Physics of Ultrasonographic Imaging, WHO press, Geneva.
21. Vincent, Wang J., 2004, Transducer.
22. Zhang, Junhua, 2008, Computer-Aided diagnosis of Cervical Lymph Nodes on Ultrasonography, Fudan University, Shanghai, China.

